# Influence of Airspace Geometry and Surfactant on the Retention of Man-Made Vitreous Fibers (MMVF 10a)

*Marianne Geiser,[1]* Matthias Matter,[1]* Isabelle Maye,[1] Vinzenz Im Hof,[2] Peter Gehr,[1] and Samuel Schürch[3]**

[1]Institute of Anatomy and [2]Institute of Pathophysiology, University of Bern, Bern, Switzerland; [3]Department of Physiology and Biophysics, University of Calgary, Calgary, Alberta, Canada

**Inhaled and deposited man-made vitreous fibers (MMVF) 10a (low-fluorine preparation of Schuller 901 insulation glass) were studied by electron microscopy in hamster lungs, fixed by intravascular perfusion within 23 ± 2 min (SD) of the initial inhalation. We found fibers on the surfaces of conducting airways and alveoli. In the airways, 89% of the fibers were totally and 11% partially covered by lining-layer material. In the alveoli, 32% of the fibers were totally submersed; others touched the alveolar wall, stuck at one end, bridging the airspace. Studies in a surface balance showed that fibers were immersed into the aqueous subphase by approximately 50% at film surface tensions of 20–25 mJ/m$^2$ and were submersed (totally immersed; i.e., totally surrounded by fluid) at approximately 10 mJ/m$^2$. Fibers were also found to be phagocytosed by macrophages. We found a substantial number of particle profiles within alveolar blood capillaries. Fiber length and alveolar geometry appear to be important limiting factors for the submersion of vitreous fibers into the lungs' surface lining layer.** *Key words:* **aerosol, airways, alveoli, deposition, hamster, man-made vitreous fibers, surface balance, surface forces, surfactant.** *Environ Health Perspect* **111:895–901 (2003). doi:10.1289/ehp.5888 available via** *http://dx.doi.org/* **[Online 9 January 2003]**

Man-made vitreous fibers (MMVF) are inorganic amorphous fibers made from glass, rock, clay, slag, or pure oxide raw material. They are used primarily for thermal and acoustic insulation. The fact that asbestos fibers are carcinogenic has led to the fear that the inhalation of vitreous fibers, which have similar size and shape, poses a serious risk to human health. The mechanisms by which fibers induce lung disease are still not completely understood. The potential toxicity of a given type of fiber is determined by dimension, durability, and fiber dose in lungs (Pott and Friedrichs 1972; Stanton and Wrench 1972). Broad ranges of inhalation studies with different fiber types have been performed and have been extensively reviewed by Hesterberg and Hart (2001). A strong relationship between biopersistence of the fiber and pathogenicity in lungs has been reported (Hesterberg et al. 1998; Kamstrup et al. 1998). Most of the tested vitreous fibers were less biopersistent and caused less pathogenicity than asbestos fibers.

Despite numerous studies with reference to pathogenicity, little is known about how inhaled vitreous fibers interact with the inner surface of the lungs immediately after their deposition. Knowledge about the mechanisms of fiber retention is important with respect to the clearance of vitreous fibers and their possible risk to human health.

The surface-lining layer in lungs consists of an aqueous phase and a surfactant film at the air–liquid interface. The continuous aqueous layer adjacent to the epithelial cells has a relatively low viscosity. The existence, thickness, and continuity of a gel phase above this periciliary layer in the various airway compartments and species have been disputed. In small airways, a thick mucus layer has never been found (Geiser et al. 1997; Gil and Weibel 1971). The surfactant film at the air–liquid interface covers the aqueous phase and it is—based on all available evidence—continuous between the alveoli and central airways (Geiser et al. 1997; Gil and Weibel 1971; Im Hof et al. 1997).

Studies *in vitro* have shown that the surfactant promotes the displacement of polystyrene particles from air into an aqueous subphase, whereby the extent of immersion depends on the surface tension of the surfactant film (Gehr et al. 1990; Schürch et al. 1990, 1993): the lower the surface tension, the greater the immersion. Furthermore, there is evidence from animal studies for the displacement of a variety of spherical particles in lungs (Geiser et al. 2000a, 2000b, 2000c). The influence of the shape of particles on their immersion into the aqueous lining layer is largely unknown.

A surface tension of 32 mJ/m$^2$ was measured in the trachea of horses (Im Hof et al. 1997), and values for expiration in alveoli were below 2 mJ/m$^2$ (Schürch et al. 1985). Very recently, evidence for surface tension values below 15 mJ/m$^2$ in the intrapulmonary conducting airways was obtained from particle deposition studies in hamsters (Geiser et al. 2000c). It is not known how different surface tension values would influence the displacement of fibers into the lining layer. The immersion of fibers into the surface-lining layer and their displacement toward the epithelium by surfactant may have consequences for fiber dissolution and/or for the clearance pathway of fibers.

To evaluate the distribution of fibers within lungs immediately after their deposition, inhaled and deposited MMVF 10a were studied in hamsters by electron microscopy. The immersion of fibers, promoted by a surfactant film formed on an aqueous substrate, was assessed in a surface balance by light microscopy.

## Materials and Methods

*Fibers.* MMVF 10a were kindly provided by Philippe Thévénaz (Research and Consulting Company, Füllinsdorf, Switzerland). They have a smooth surface and are mostly straight cylinders (Figure 1).

To estimate the surface free energy of the glass fibers used in this study, we measured the contact angle of dibutyl phthalate droplets (surface tension, 34.5 mJ/m$^2$ at 22°C) placed on glass slides cleaned with chromic acid at different time points after exposure to laboratory air. The contact angle of dibutyl phthalate droplets on glass was compared with that obtained on a polystyrene substrate with the same fluid. In addition, the solid-vapor free energy was estimated by using the equation of state approach (Spelt and Li 1996). The equation of state helps determine the solid-vapor interfacial energy from the measured contact angle that a test fluid droplet of a known surface tension makes on a solid substrate.

***Animals, aerosol generation, and inhalation.*** Inhaled and deposited fibers were studied in male Syrian Golden hamsters [$n$ = 4; AURA, HanIbm:AURA (specific–pathogen free); Biological Research Laboratories Ltd., Füllinsdorf, Switzerland] weighing 132–163 g. The animals, aerosol generation, and inhalation have been described in detail previously (Geiser et al. 2000a; Im Hof et al. 1989; Waber et al. 1999). Briefly, aerosols were

Address correspondence to M. Geiser, Institute of Anatomy, Division of Histology, University of Bern, Bühlstrasse 26, CH-3000 Bern 9, Switzerland. Telephone: 41-31-631-8475. Fax: 41-31-631-3807. E-mail: geiser@ana.unibe.ch

*M.G., M.M., and S.S. contributed equally to this work. We thank P. Thévénaz for providing the vitreous fibers and S. Frank, B. Kupferschmid, B. Krieger, T. Weissbach, and K. Babl for excellent technical assistance.

This work was supported by Swiss National Science Foundation grant 32-65352.01, Canadian Institutes of Health Research, the Alberta Heritage Foundation for Medical Research, and the Silva Casa Foundation.

The authors declare they have no conflict of interest.

Received 16 July 2002; accepted 8 January 2003.

generated by jet nebulization of droplets of suspensions of MMVF 10a fibers (2 mg/mL in 100% ethanol) into a particle-free air stream. The fibers were then dried, charge equilibrated, and concentrated before being injected into a reservoir and transferred to the inhalation/exhalation channel. The deeply anesthetized and completely relaxed hamsters inhaled the aerosol directly from the reservoir through an intratracheal cannula during continuous negative-pressure ventilation. They were ventilated with a tidal volume ($V_T$) of 0.95 ± 0.06 mL (mean ± SD)—maintained at 70–80% of total lung capacity—and a breathing frequency ($f$) of 61 ± 1 breath/min (mean ± SD), which equals slow, deep breathing (Inglis 1980). The breathing parameters and the number of inhaled and exhaled fibers were measured by pneumotachography and laser-light scattering photometry. Because the fibers used in this study were heterogeneous in size, number estimates are of directional value only. Aerosols were inhaled for 5–12 min, until a sufficient number of fibers for microscopic analysis were deposited. Immediately thereafter, the lungs were prepared for intravascular perfusion fixation.

We collected aerosol samples on filters and analyzed the fiber size distribution (Figure 2). The average length of 200 fibers measured by light microscopy was 16 ± 13 µm (mean ± SD; range, 1–66 µm); the average diameter was 1.1 ± 0.2 µm (range, 0.6–1.7 µm). The average length-to-diameter ratio was 15.6 ± 13.3 (range, 1.1–64.0). Twenty fibers had a length-to-diameter ratio of < 3; hence, the particulate fraction of MMVF 10a in the aerosol was 10%.

***Lung fixation.*** Whole lungs can be preserved for morphologic analysis by the introduction of a suitable fixative into the airways of a collapsed lung or by delivery of the fixatives to the lungs via the blood vessels (Weibel 1984). The instillation of aqueous fixative solutions into the airways is not suitable for the investigation of the inner surface of the lungs because the surface-lining layer and all its cellular and acellular constituents are dislocated from their native positions and transferred to other regions of the organ (Brain et al. 1984). Instillation of airways with nonpolar fixative solutions (1% osmium tetroxide dissolved in perfluorocarbon) has been demonstrated to preserve the aqueous lining layer and especially also the surfactant film at the air–liquid interface (Geiser et al. 1997; Lee et al. 1995; Sims et al. 1991; Thurston et al. 1976). However, it is not known whether material that is not submersed in the surface-lining layer may be dislocated by this procedure.

Because it was the aim of this study to investigate the location of deposited fibers with respect to the inner surface of the lungs, the fixative solutions were applied by vascular perfusion via the pulmonary artery, which allows the airways and alveoli to remain in their natural air-filled state. Sequential intravascular perfusion of buffered 2.5% glutaraldehyde, 1% osmium tetroxide, and 0.5% uranyl acetate (Bachofen et al. 1982; Im Hof et al. 1989; Weibel 1984) has been shown to well preserve the surface-lining layer with its phagocytic cells and the surfactant film at the air–liquid interface of intrapulmonary conducting airways and alveoli in laboratory animals (Geiser et al. 1997; Gil and Weibel 1969, 1971).

All lungs were fixed within 23 ± 2 min of the initial inhalation. The short time between inhalation and lung fixation allows the investigation of fibers as close as possible to where they were deposited. After fixation, the lungs were removed from the thorax and split into left lung, right lung, and accessory lobe (Geiser et al. 1990).

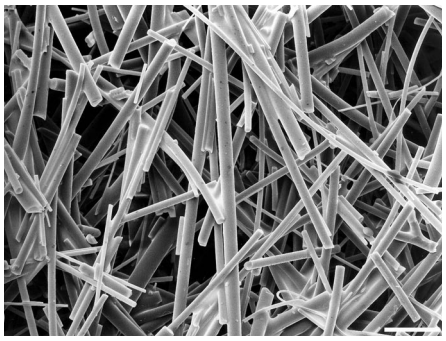

**Figure 1.** Scanning electron micrograph of the fibers as they were used for aerosol generation. They have a cylindrical shape and are of variable lengths and diameters. Bar = 10 µm.

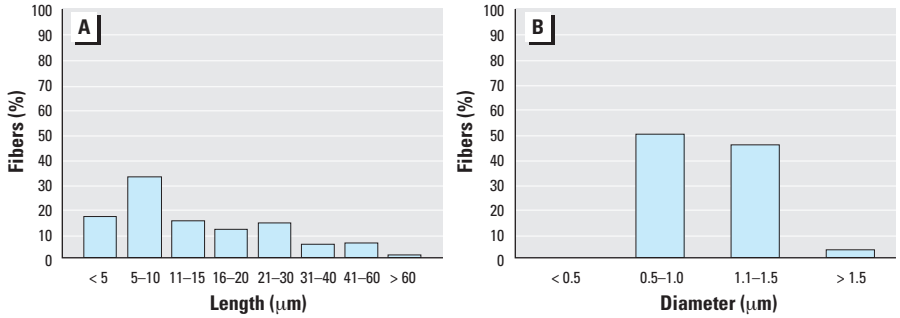


**Figure 2.** Size distributions of MMVF 10a in the aerosol; the fibers ($n$ = 200) were measured on light micrographs.

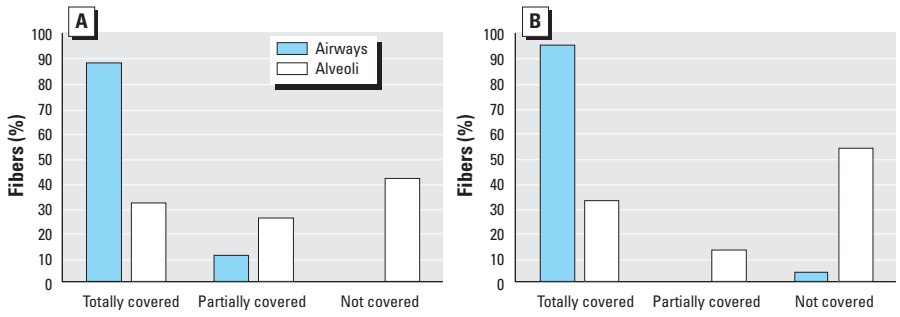


**Figure 3.** SEM (*A*) and TEM (*B*) analysis of fibers retained on the surfaces in the intrapulmonary conducting airways and in the alveoli (defined by amount of lung lining-layer material covering fibers).

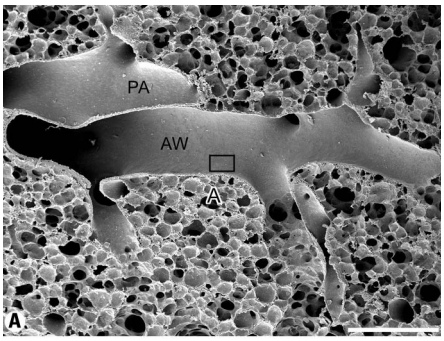


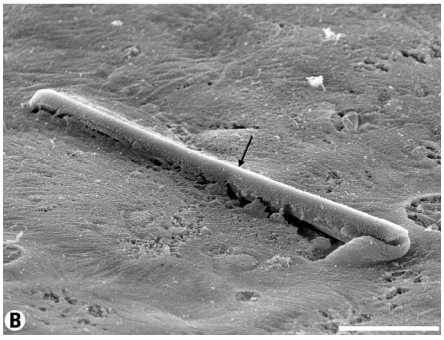


**Figure 4.** Scanning electron micrograph of a fiber retained in an intrapulmonary conducting airway. (*A*) Overview of the retention site (boxed area); bar = 500 µm. Abbreviations: A, alveoli; AW, intrapulmonary conducting airway; PA, pulmonary artery. (*B*) The fiber is completely covered by the surface-lining layer (arrow); bar = 5 µm.

***Tissue processing for microscopic analysis.*** The lung lobes were cut perpendicularly to the longitudinal axis into series of thick (3 mm) and thin (1.5 mm) slices, with random start (Geiser et al. 1990). The thin slices were used for electron microscopy, and the thicker ones for other purposes. A total of 49 thin slices were sampled for transmission electron microscopy (TEM) and further cut into cubes of about 1 mm side length. These tissue blocks ($n$ = 144) were dehydrated in ethanol and embedded in Epon (Im Hof et al. 1989). Ultrathin sections, stained with uranyl acetate and lead citrate, were examined with a Philips 300 transmission electron microscope (Philips AG, Zürich, Switzerland) operating at 60 kV.

For scanning electron microscopic (SEM) analysis, a total of 15 thin slices were sampled, dehydrated in ethanol, critical-point-dried, and sputter-coated with platinum. They were examined with a Philips XL 30-FEG scanning electron microscope (Philips) operating at 10 kV. Length and diameter of all registered fibers were measured by SEM.

***Displacement of MMVF 10a in the Langmuir-Wilhelmy balance.*** The displacement of MMVF 10a fibers into an aqueous substrate by a surfactant film was investigated with a monolayer of 1,2-dipalmitoyl-sn-3-glycerophosphatidylcholine (DPPC; Sigma-Aldrich Canada Ltd., Oakville, Ontario, Canada) in a Langmuir-Wilhelmy surface balance (our own design). The DPPC monolayer was spread from a solution of 2 mg/mL in ethanol onto an aqueous substrate of a solution of 0.9% NaCl and 40% sucrose (density, 1.25 g/mL). The monolayer was spread within an area of 25 $cm^2$ enclosed by a Teflon ribbon supported by a rhombic frame (Schoedel et al. 1969). Our objective was to assess the displacement of glass fibers at surface tensions between 30 and 5 $mJ/m^2$. Pulling the rhombic frame to an elongated shape reduced the surface tension of the DPPC film, and the surface tension force was measured by a platinum Wilhelmy plate connected to an electrobalance.

After adjustment of the monolayer surface tension to a preset value, the glass dish was placed onto a microscope stage and fibers were blown onto the monolayer. The fibers were then observed and photographed with a Nikon Optiphot metallurgical microscope (Nikon, Mississauga, Ontario, Canada), equipped for differential interference contrast and dark field for epi-illumination.

## Results

***Fibers retained on the surfaces of airways and alveoli: SEM analysis.*** The analysis by SEM allowed the investigation of fibers on airway and alveolar surfaces. Single fibers and small aggregates were found. Larger aggregates were observed at bifurcations. In the intrapulmonary conducting airways, 89% of the fibers were found to be completely covered by surface-lining layer material, and 11% were only partially covered (Figures 3 and 4). The average length and diameter of the fibers in the airways were 37.3 ± 19.4 µm (mean ± SD; range, 7–104 µm) and 1.1 ± 0.4 µm (range, 0.3–2 µm), respectively (Figure 5). The average length-to-diameter ratio was 34.0 ± 19.0 (range, 7–122).

In the alveoli, 32% of the fibers were completely covered, 26% were partially, and 42% were not covered by the lung-lining layer (Figures 3 and 6). Some fibers appeared to project into the alveolar airspace or to cross it, and they touched the alveolar surface only with their ends. The average length and diameter of the fibers in the alveoli were 20.9 ± 8.3 µm (range, 9–35 µm) and 0.9 ± 0.3 µm (range, 0.5–1.5 µm), respectively (Figure 5). The average length-to-diameter ratio was 27.8 ± 14.0 (range, 10–52).

***Fiber retention in lungs by TEM.*** The analysis by TEM allowed the investigation of fibers within the entire lung tissue. Because with this method we analyzed two-dimensional transects of the fibers in tissue sections, we could observe the traces of cut cylinders, which were in all cases either circles or ellipses (Mattfeldt et al. 1994). A vitreous glass profile with irregular complicated shape can only originate from a broken fiber. Furthermore, if the profile's length-to-diameter ratio is also < 3, it is most likely a profile of a particle.

From the 144 embedded tissue blocks, 96 contained intrapulmonary conducting airways as well as lung parenchyma, and these were used for analysis by TEM. A total of 335 MMVF 10a profiles, which are electron-dense and easy to recognize, were analyzed on micrographs of ultrathin sections (Table 1). We found 35 mostly fiber profiles in the conducting airways, and we registered 69 profiles in the alveoli, about half of them originating from fibers and the other half from particles. Eight fibers and/or particles were found to be phagocytosed by airway macrophages (Figure 7B),

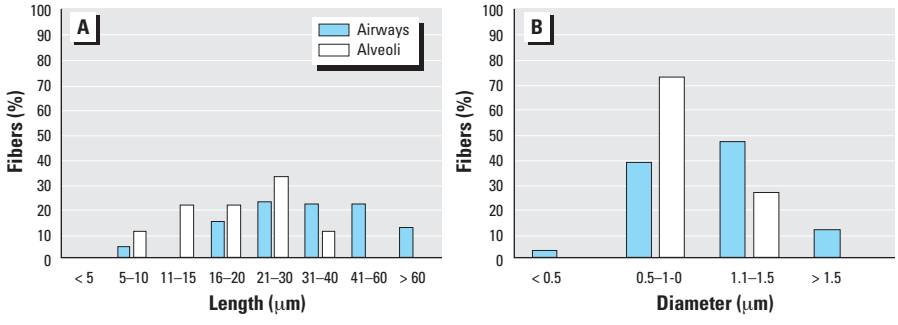


**Figure 5.** Size distribution of fibers retained on the surfaces of intrapulmonary conducting airways and alveoli analyzed by SEM. (*A*) The lengths of 73 fibers (64 in airways and 9 in alveoli) were measured; 9 fibers in airways and 10 fibers in alveoli could not be measured because one fiber end was not visible. (*B*) The diameters of 91 fibers (72 in airways, 19 in alveoli) were measured; the diameter of one fiber in the airways could not be measured.

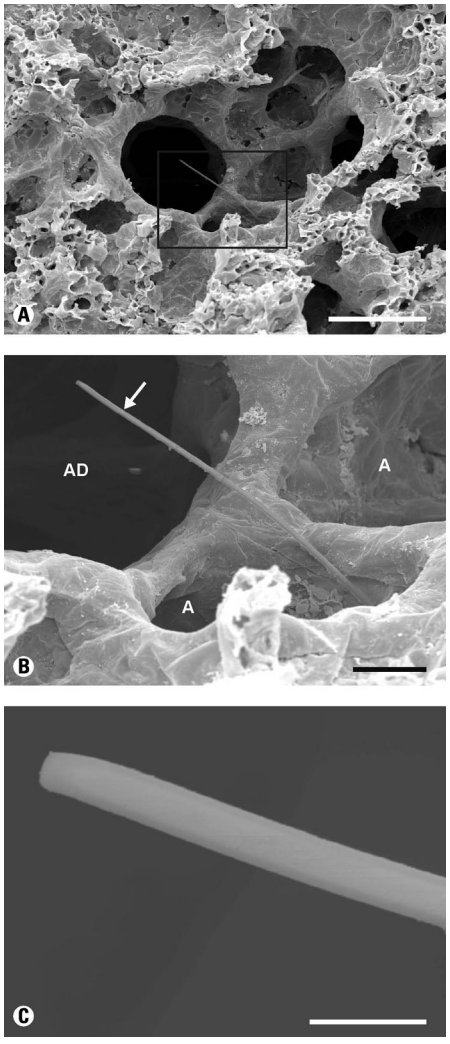


**Figure 6.** Scanning electron micrographs of a fiber retained in the gas exchange compartment. (*A*) Overview of the retention site (boxed area); bar = 50 µm. (*B*) The fiber touched the alveolar wall with one fiber end only; the other end (arrow) projects into the airspace; bar = 10 µm. Abbreviations: A, alveoli; AD, alveolar duct. (*C*) The fiber end that did not come into contact with the alveolar surface was not covered by lung lining-layer material; bar = 2 µm.

and nine by alveolar macrophages (Figure 8C). We observed 228 mostly particle profiles in the lumen of alveolar blood capillaries, and 1 within a pulmonary artery. One fiber profile was found within a type I epithelial cell, and the location of another one could not be identified. Neither fiber nor particle profiles were found in the interstitium.

In airways, 96% of the profiles were submersed in the surface-lining layer, whereas 4% appeared not to be covered by any material (Figures 3 and 7A). In alveoli, 33% of the profiles were found to be completely, 13% partially, and 54% not covered by any surface-lining layer material (Figures 3, 8A, and 8B). The profiles found in the lumina of blood vessels had blank surfaces (Figure 8D).

***Displacement of fibers into an aqueous substrate by a surfactant film.*** The experiments in the Langmuir-Wilhelmy surface balance demonstrated that the extent of fiber immersion into the aqueous phase depends on the surface tension of the film at the air–liquid interface. At 30 mJ/m$^2$, < 10% of the fibers were submersed into the aqueous substrate, whereas at surface tensions < 20 mJ/m$^2$, almost all fibers (> 95%) were completely submersed (Figure 9). However, the displacement of fibers was found to depend also on size. Fibers shorter than 10 µm were immersed into the aqueous subphase by approximately 50% at 25–30 mJ/m$^2$ and were completely submersed at ≤ 20 mJ/m$^2$. Fibers with a length of 20–30 µm were immersed to 50% at a surface tension of 15 mJ/m$^2$ and to 95% at ≤ 10 mJ/m$^2$.

***Surface free energy of glass fibers.*** The surface free energy of clean glass is several hundred millijoules per square meter. However, glass surfaces adsorb impurities (materials) suspended in the ambient air, which considerably reduces the surface free energy value of glass. Measurements on surfaces of glass slides have demonstrated that clean glass, after exposure for 15–20 hr to laboratory air, has a surface free energy close to that of polystyrene (i.e., ~ 35 mJ/m$^2$). We therefore expect that the glass fibers investigated in the anatomy laboratory in Bern had surface free energies similar to that of polystyrene.

## Discussion

The microscopic analyses of inhaled and deposited MMVF 10a in hamster lungs described here show that in the conducting airways almost all fibers were submersed in the aqueous lining layer, whereas in the alveoli only about one-third of the fibers were completely covered by lining layer material. It has been shown previously that the displacement of polystyrene microspheres depends on the surface tension of the surfactant film at the air–liquid interface (Gehr et al. 1990; Schürch et al. 1990, 1993). The lower the film surface tension, the greater the extent of particle immersion into the aqueous subphase. The extent of immersion as assessed in the Langmuir-Wilhelmy surface balance demonstrated that immersion of MMVF 10a into the subphase by approximately 50% occurred for fibers shorter than 10 µm at film surface tensions of 25 mJ/m$^2$ and for those 20–30 µm in length at 15 mJ/m$^2$. For submersion of the longer fibers, the film surface tension had to be ≤ 10 mJ/m$^2$.

The calculation of the forces that are exerted on cylindrical MMVF 10a after their deposition on a liquid surface is somewhat more difficult than that for forces exerted on microspheres, because of the complex wetting behavior. First, fibers have infinite possibilities with respect to their orientation of hitting a liquid surface. Second, MMVF 10a have variable dimensions and are straight or bent cylinders, meaning that forces exerted on them would have to be calculated for each single fiber. Third, the surface chemistry of the glass fibers does not seem to be homogeneous, in that the three-phase line (the line where the vapor, fluid, and solid phases join) appears to be corrugated. This can be observed by light microscopy, especially on long fibers; dry spots (not wetted by the surfactant film) are followed by partially immersed parts, and so on (Figure 10). From the model experiments in the Langmuir-Wilhelmy surface balance, it follows that glass fibers (MMVF 10a) are displaced into the aqueous lung-lining layer only below a film surface tension of 20 mJ/m$^2$. Assuming that clean glass has a surface free energy of several hundred millijoules per square meter, one would expect immediate wetting and submersion of glass fibers caused by a surfactant film of a surface free energy of approximately 25 mJ/m$^2$. However, glass surfaces tend to adsorb impurities (materials) suspended in the ambient air, such that the surface free energy of the fibers used in this study is expected to be considerably lower. As a consequence, we observed that such fibers are wetted and displaced only if the film surface tension falls below approximately 30 mJ/m$^2$, which is consistent with a reduced surface free energy of the glass due to adsorption of impurities.

According to microscopic analysis, about 90% of the glass fibers were submersed in the surface-lining layer in the intrapulmonary conducting airways. In this lung compartment, fiber length seemed not to be a limiting factor for their displacement, because fibers up to 104 µm in length were found to be submersed. The *in vitro* experiments demonstrated that in order to promote total immersion of glass fibers of a length of 20–30 µm, the film surface

**Table 1.** Distribution of MMVF 10a in hamster lungs by TEM and shape profiles.

| | Localization of MMVF 10a profiles | | Shape profiles in TEM sections (%) | | |
|---|---|---|---|---|---|
| Lung compartment | No.[a] | Percent | Elliptical/ circular | Partially elliptical | Angular surface |
| Intrapulmonary airways | 35 | 10.5 | | | |
| Free[b] | 27 | 8.1 | 29.6 | 59.3 | 11.1 |
| Phagocytosed[c] | 8 | 2.4 | 25 | 50 | 25 |
| Alveoli | 69 | 20.6 | | | |
| Free[b] | 60 | 17.9 | 13.3 | 31.7 | 55.0 |
| Phagocytosed[c] | 9 | 2.7 | 11.1 | 22.2 | 66.7 |
| Type I cell | 1 | 0.3 | 0 | 100 | 0 |
| Endothelial cell | 0 | 0 | 0 | 0 | 0 |
| Alveolar blood capillary[d] | 228 | 68.0 | 0 | 11.4 | 88.6 |
| Pulmonary artery[d] | 1 | 0.3 | 0 | 0 | 100 |
| Interstitium | 0 | 0 | 0 | 0 | 0 |
| Unidentified location | 1 | 0.3 | 0 | 100 | 0 |
| Total | 335 | 100 | | | |

[a]Number of MMVF 10a profiles analyzed on TEM micrographs. [b]Fiber or particle profiles on lung surfaces, not within any cell. [c]Fiber or particle profiles engulfed by macrophages on lung surfaces. [d]Profiles within lumen of blood vessels.

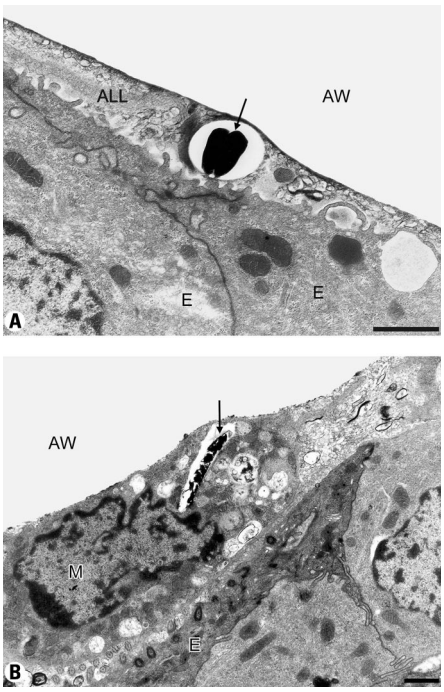


**Figure 7.** Transmission electron micrographs of fiber profiles (arrows) in intrapulmonary conducting airways. (*A*) The fiber was submersed in the aqueous lining layer (ALL). (*B*) Fiber phagocytosed by airway macrophage (M). Abbreviations: AW, airway lumen; E, epithelium. Bars = 1 µm.

tension has to fall to approximately 10 mJ/m$^2$. This value is considerably below the surface tension of 32 mJ/m$^2$ measured in the trachea of horses (Im Hof et al. 1997) and substantially below the equilibrium surface tension of approximately 25 mJ/m$^2$ for pulmonary surfactant films. Because surface tensions < 22–25 mJ/m$^2$ can only be achieved by mechanically compressed films, the conclusion is that the surfactant film reaches at least temporarily a compressed state in the intrapulmonary conducting airways of hamsters. Because the alveolar surfactant film reaches minimum surface tensions below approximately 2 mJ/m$^2$ under *in vivo* conditions (Bachofen et al. 1987), it is clear that there must be a surface tension gradient between the compressed alveolar surfactant film and that in the trachea or large bronchi, but the definition of the gradient remains unclear.

Direct surface tension measurements in the small airway compartments have not been possible so far with current techniques because these airways are not accessible. However, indirect evidence for surface tensions far below the equilibrium value of approximately 25 mN/m in the central airways of rabbits has recently been obtained by Bachofen and Schürch (2001), who demonstrated that the shape of bronchiolar macrophages beneath the surfactant film in the surface-lining layer depends on the local surface tension. The shape of the macrophages, determined by TEM, may serve in turn to estimate the airway surface tension at that location.

Because the surface tension in the alveoli reaches values < 2 mJ/m$^2$ on expiration, one would expect all of the fibers in the alveoli to be completely submersed in the surface-lining layer. However, in the present study, we found that about one-third of the fibers in alveoli were not covered by the surface-lining layer. This may be due to geometric limitations. The geometry of alveoli in hamsters resembles spherical cavities with an average diameter of about 80 µm (Kennedy et al. 1978). Long fibers may touch the inner surface with the tips of both ends and bridge the alveolar airspace. Such configurations have been observed (Rogers et al. 1999). The fibers are immersed into the lining layer only at their ends. Therefore, partial coverage of fibers by lung lining material as observed by SEM may be explained by size and geometry of the fibers and the airspaces.

Dissolution of the fibers becomes possible after their displacement into the aqueous lining layer. In addition, it is likely that surfactant

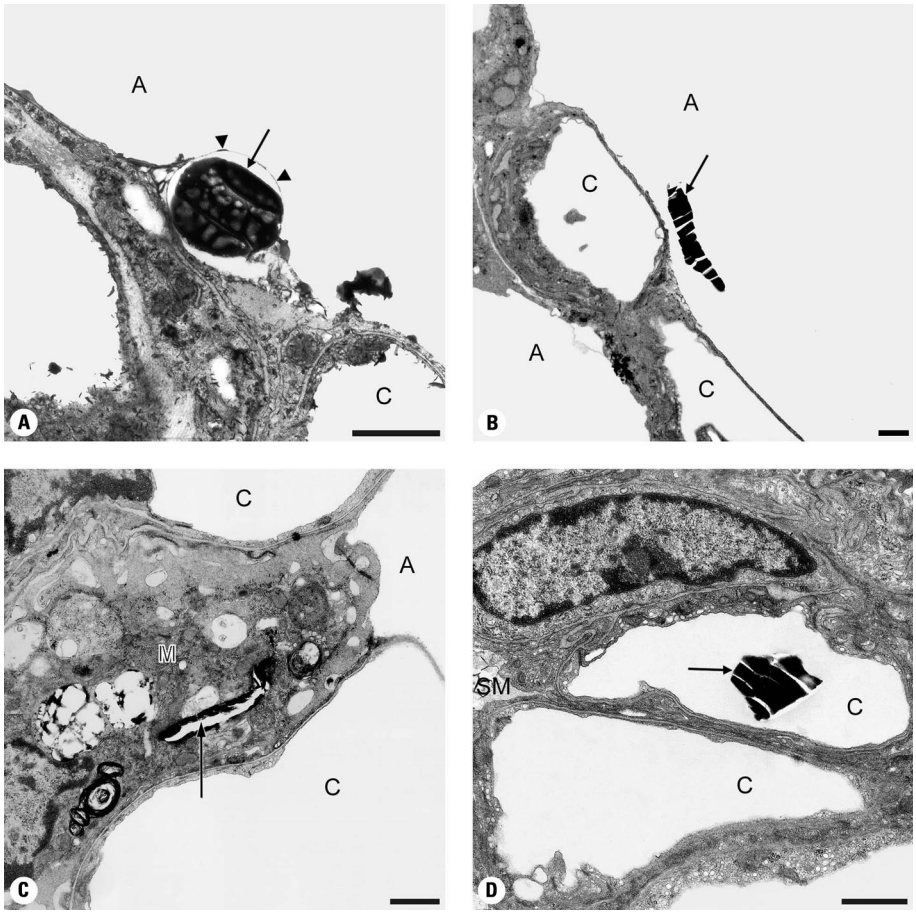


**Figure 8.** Transmission electron micrographs of MMVF 10a profiles (arrows) retained in the lung parenchyma. Abbreviations: A, alveolar lumen; C, blood capillary; SM, surfactant material in adjacent alveolus. (*A*) Submersed fiber profile. Note the surfactant film (arrowheads) at the air–liquid interface. (*B*) Fiber profile not covered by any surface-lining layer material. The fiber is located some distance from the epithelium. (*C*) Fiber profile within an alveolar macrophage (M). (*D*) Particle profile in the lumen of an alveolar blood capillary; the surface of the irregularly shaped profile is blank (no other material at the interface). Bars = 1 µm.

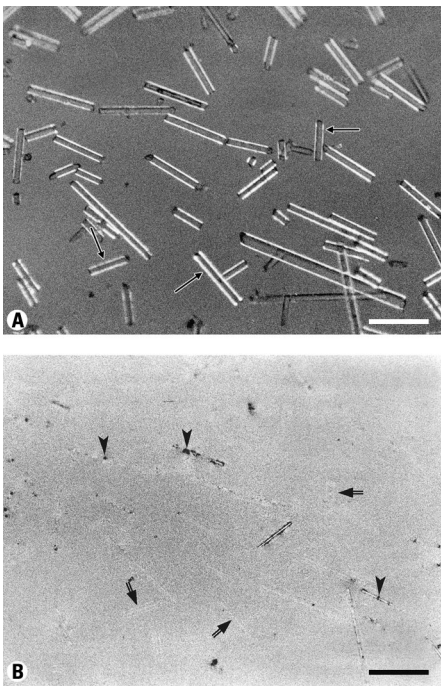


**Figure 9.** Light micrographs of MMVF 10a deposited on DPPC film at a surface tension of 15 mJ/m$^2$ in a Langmuir-Wilhelmy surface balance. (*A*) Micrograph taken with epi-illumination and dark-field optics. All of the fibers, regardless of whether they are completely wetted (arrows) or only partially wetted, are visible. (*B*) Differential interference contrast micrograph for epi-illumination of same fibers as in (*A*). Double arrows indicate totally submersed fibers, not visible with differential interference contrast. Note the occurrence of infrequent nonhomogeneous wetting, shown as dark spots (arrowheads). See also Figure 10. Bars = 10 µm.

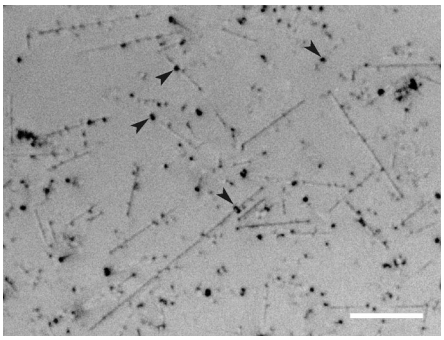

**Figure 10.** Micrograph of MMVF 10a deposited onto DPPC film in a Langmuir-Wilhelmy surface balance at a surface tension of 30 mJ/m$^2$. Fibers appear partially immersed into the aqueous substrate. Nonhomogeneous wetting is shown as dark spots (arrowheads), which represent dry "islands" along most of the fibers. Bar = 10 µm.

components or proteins are adsorbed onto the surfaces of the fibers, which may alter their clearance pathway or their toxicologic potency.

The displacement of fibers into the surface-lining layer brings them into close contact with resident macrophages, which comprise a major clearance pathway for particles deposited in the alveoli and in small airways (Geiser et al. 1990, 2000a, 2000b). In addition, the displacement of fibers toward the epithelium may facilitate particle uptake by epithelial cells and eventually translocation to interstitial and endothelial sites, which may have consequences for causing lung disease.

In the present study, about two-thirds of all vitreous glass profiles were found in the lumen of alveolar blood capillaries. The majority of these profiles had irregular shapes and angular surfaces and most likely represents particles originating from broken fibers. The particulate fraction of MMVF 10a in the aerosol was 10%. Such particles are in a size range to reach the alveoli by inhalation and to be deposited there. This is demonstrated by the observation that many more particle profiles were found in the alveolar than in the airway compartment. Currently, it is not known how the MMVF 10a particles entered the capillary lumen. There are several mechanisms by which particles can be displaced from one tissue compartment to another one. First, particles < 1 μm in diameter or those persisting on lung surfaces have been shown to be taken up more readily by epithelial cells (Ferin et al. 1992; Mossmann et al. 1978) or to be translocated even to interstitial and endothelial sites (Oberdörster et al. 1996). We found only one vitreous glass profile within the interalveolar septum, within a type I epithelial cell. Therefore, clearance of MMVF 10a through the epithelial cells and further translocation via the interstitium and endothelial cells into the lumen of blood capillaries is unlikely. This is consistent with observations of Brody et al. (1981), who showed that for minute asbestos fibrils in rats, the above-mentioned sequence of particle transport had occurred only 4 or more days after exposure. In contrast, in the present study, < 1 hr elapsed between the onset of the inhalation until lung fixation. Second, mechanical translocation (e.g., due to the formation of a pneumothorax) is another mechanism by which intact or broken fibers may have entered the blood circulation. Asbestos and glass fibers piercing the air–blood barrier have been demonstrated by others (Lee et al. 1979; Rogers et al. 1999). In the present study, this might have happened upon pneumothorax formation, but we did not see ruptured tissue near to the location where we found fibers. Finally, particles may be driven through the cell membranes, for example, through those of the type I epithelial cells, by interfacial forces (adhesive interactions). We demonstrated in a recent study (Rothen et al. In press) that particles < 1 μm in diameter are able to penetrate the cell membrane of erythrocytes by nonspecific mechanisms. These observations are consistent with those made by Rimai et al. (2000), who showed that spherical glass particles in the micrometer size range are driven into a polystyrene substrate by adhesive interactions. For example, glass particles 4 μm in radius become engulfed by the substrate by approximately 90%, whereas particles 10 μm in radius become substantially less engulfed. These investigators discussed the possibility of total engulfment of relatively hard and small particles by a softer substrate.

Nevertheless, if the particulate fraction of MMVF 10a is cleared by the blood circulation, organs beyond the lungs should be carefully investigated after fiber exposure. Marsh et al. (1990) reported a significant increase in mortality for nephritis and nephrosis in the 1985 follow-up study of workers exposed to man-made mineral fibers. Sali et al. (1999) suggested the possibility of an increased risk of nonmalignant renal disease with duration of employment in a nonneoplastic mortality study of European workers who produced rock or slag wool. Moreover, they demonstrated that mortality from ischemic heart disease was increased in workers exposed to rock or slag wool and in continuous-filament workers. Yet, Sjögren (2000) suggested that the increased mortality from ischemic heart disease originates from the high concentration of fibrinogen caused by the low-grade inflammation after fiber inhalation, and Chiazze et al. (1999) did not find any association between respirable fibers and nephritis or nephrosis in a case–control study on Caucasians who worked in glass wool production plants.

The observation that fibers were preferentially deposited at bifurcations in airways and alveoli has also been reported for inhalation studies using other fiber types (Brody et al. 1981; Brody and Roe 1983; Rogers et al. 1999).

In summary, the present study shows that glass fibers are displaced by a surfactant film and immersed into the aqueous lining layer in airways and alveoli, if the surface tension reaches ≤ 10 mJ/m$^2$, provided that the fibers come into contact with the inner surface of the lung. The geometry and dimension of the airspace and the fibers are therefore important factors for fiber retention. We conclude that the sequence of wetting and immersion of inhaled and deposited MMVF 10a fibers into the aqueous lining layer by the surfactant film at the air–liquid interface is similar to that of spherical particles and is crucial for the retention of any kind of particles and fibers. Particles of identical shape, including asbestos or ceramic fibers, may have a surface free energy similar to that of vitreous fibers under ambient conditions. Presumably, they are likewise displaced into the aqueous lining layer after their deposition in the lungs. Therefore, the increased pathogenicity of certain fibers can most likely not be explained by different retention mechanisms. Adsorption of surfactant components or proteins upon displacement into the aqueous phase by surfactant is possible and needs further investigation because it may be a crucial factor for health effects. In addition, the importance of clearance of the particulate fraction via the blood stream needs further investigation.

## References


Bachofen H, Ammann A, Wangensteen D, Weibel ER. 1982. Perfusion fixation of lungs for structure-function analysis: credits and limitations. J Appl Physiol 53:528–533.

Bachofen H, Schürch S. 2001. Alveolar surface forces and lung architecture. Comp Biochem Physiol A 129:183–193.

Bachofen H, Schürch S, Urbinelli M, Weibel ER. 1987. Relations among alveolar surface tension, surface area, volume and recoil pressure in rabbit lungs. J Appl Physiol 62:1878–1887.

Brain JD, Gehr P, Kavet I. 1984. Airway macrophages. The importance of the fixation method. Am Rev Respir Dis 129:823–826.

Brody AR, Hill LH, Adkins B, O'Connor RW. 1981. Chrysotile asbestos inhalation in rats: deposition pattern and reaction of alveolar epithelium and pulmonary macrophages. Am Rev Respir Dis 123:670–679.

Brody AR, Roe MW. 1983. Deposition pattern of inorganic particles at the alveolar level in the lungs of rats and mice. Am Rev Respir Dis 128:724–729.

Chiazze L, Watkins DK, Fryar C, Fayerweather W, Bender JR, Chiazze M. 1999. Mortality from nephritis and nephrosis in the fibreglass manufacturing industry. Occup Environ Med 56:164–166.

Ferin J, Oberdörster G, Penney DP. 1992. Pulmonary retention of ultrafine and fine particles in rats. Am Respir Cell Mol Biol 6:535–542.

Gehr P, Schürch S, Berthiaume Y, Im Hof V, Geiser M. 1990. Particle retention in airways by surfactant. J Aerosol Med 3:27–43.

Geiser M, Cruz-Orive LM, Im Hof V, Gehr P. 1990. Assessment of particle retention and clearance in the intrapulmonary conducting airways of hamster lungs with the fractionator. J Microsc 160:75–88.

Geiser M, Gerber P, Maye I, Im Hof V, Gehr P. 2000a. Retention of Teflon particles in hamster lungs: a stereological study. J Aerosol Med 13:43–55.

Geiser M, Im Hof V, Siegenthaler W, Grunder R, Gehr P. 1997. Ultrastructure of the extracellular lining layer in hamster airways: is there a two-phase system? Micros Res Techn 36:428–437.

Geiser M, Leupin N, Maye I, Im Hof V, Gehr P. 2000b. Interaction of fungal spores with the lungs: distribution and retention of inhaled *Calvatia excipuliformis* spores. J Allergy Clin Immunol 106:92–100.

Geiser M, Schürch S, Im Hof V, Gehr P. 2000c. Retention of particles: structural and interfacial aspects. In: Particle-Lung Interaction. Lung Biology in Health and Disease Series, Vol 143 (Gehr P, Heyder J, eds). New York: Marcel Dekker, 291–322.

Gil J, Weibel ER. 1969. Improvements in demonstration of lining layer of lung alveoli by electron microscopy. Respir Physiol 8:13–36.

———. 1971. Extracellular lining of bronchioles after perfusion-fixation of rat lungs for electron microscopy. Anat Rec 169:185–200.

Hesterberg TW, Chase G, Axten C, Miller WC, Musselmann RP, Kamstrup O, et al. 1998. Biopersistence of synthetic vitreous fibres and amosite asbestos in the rat lung following inhalation. Toxicol Appl Pharmacol 151:262–275.

Hesterberg TW, Hart GA. 2001. Synthetic vitreous fibers: a review of toxicology research and its impact on hazard classification. Crit Rev Toxicol 31:1–53.

Im Hof V, Gehr P, Gerber V, Lee MM, Schürch S. 1997. In vivo determination of surface tension in the horse and in vitro model studies. Respir Physiol 109:81–93.

Im Hof V, Scheuch G, Geiser M, Gebhart J, Gehr P, Heyder J. 1989. Techniques for the determination of particle deposition in lungs of hamsters. J Aerosol Med 2:247–259.

Inglis JK. 1980. Introduction to Laboratory Animal Science and Technology. Oxford, UK:Pergamon Press.

Kamstrup O, Davis JMG, Ellehauge A, Guldberg M. 1998. The biopersistence and pathogenicity of man-made vitreous fibers after short- and long-term inhalation. Ann Occup Hyg 42:191–199.

Kennedy AR, Desrosiers A, Terzaghi M, Little JB. 1978. Morphometric and histological analysis of the lungs of Syrian golden hamsters. J Anat 125:527–553.

Lee KP, Barras CE, Griffith FD, Waritz RS. 1979. Pulmonary response to glass fibre by inhalation exposure. Lab Invest 40:123–133.

Lee MM, Schürch S, Roth SH, Jiang X, Cheng S, Bjarnason S, et al. 1995. Effect of acid aerosol exposure on the surface properties of airway mucus. Exp Lung Res 21:835–851.

Marsh GM, Enterline PE, Stone RA. 1990. Mortality among a cohort of US man-made mineral fibres workers: 1985 follow-up. J Occup Med 32:594–604.

Mattfeldt T, Clarke A, Archenhold G. 1994. Estimation of the directional distribution of spatial fibre processes using stereology and confocal scanning laser microscopy. J Microsc 173:87–101.

Mossmann BT, Adler KB, Craighead JE. 1978. Interaction of carbon particles with tracheal epithelium in organ culture. Environ Res 16:110–122.

Oberdörster G, Finkelstein J, Ferin J, Godleski JJ, Chang LY, Gelein R, et al. 1996. Ultrafine particles as a potential environmental health hazard. Chest 109:S68–S69.

Pott F, Friedrichs KH. 1972. Tumoren der Ratte nach i.p.-Injektion faserförmiger Stäube [in German]. Naturwissenschaften 59:318.

Rimai DS, Quesnel DJ, Busnaina AA. 2000. The adhesion of dry particles in the nanometer to micrometer size range. Colloid Surf A Physicochem Engin Aspects 165:3–10.

Rogers RA, Antonini JM, Brismar H, Lai J, Hesterberg TW, Oldmixon EH, et al. 1999. *In situ* microscopic analysis of asbestos and synthetic vitreous fibers retained in hamster lungs following inhalation. Environ Health Perspect 107:367–375.

Rothen B, Schürch S, Gehr P. In press. Confocal scanning microscopy to study the interaction of fine and ultrafine particles with pulmonary cells. Am J Respir Crit Care Med.

Sali D, Boffetta P, Andersen A, Cherrie JW, Change Claude J, Hansen J, et al. 1999. Non-neoplastic mortality of European workers who produce man made vitreous fibres. Occup Environ Med 56:612–617.

Schoedel W, Slama H, Hansen E. 1969. Zeitabhängige Veränderungen des Filmdruckes alveolärer Oberflächenfilme im Langmuir-Trog [in German]. Pfluegers Arch 306:20–32.

Schürch S, Bachofen H, Weibel ER. 1985. Alveolar surface tension in excised rabbit lungs: effect of temperature. Respir Physiol 62:31–45.

Schürch S, Gehr P, Im Hof V, Geiser M, Green F. 1990. Surfactant displaces particles toward the epithelium in airways and alveoli. Respir Physiol 80:17–32.

Schürch S, Geiser M, Gehr P. 1993. Surface properties and function of alveolar and airway surfactant. In: Biosurfactants (Kosaric N, ed). New York:Marcel Dekker, 287–304.

Sims DE, Westfall JA, Kiorpes AL, Horne MM. 1991. Preservation of tracheal mucus by nonaqueous fixative. Biotech Histochem 66:173–180.

Sjögren B. 2000. Non-neoplastic mortality of European workers who produce man made vitreous fibres [Letter]. Occup Environ Med 57:284.

Spelt JK, Li D. 1996. The equation of state approach to interfacial tension. In: Applied Surface Thermodynamics. Surfactant Science Series, Vol. 63 (Neumann AW, Spelt JK, eds). New York:Marcel Dekker, 239–292.

Stanton MF, Wrench C. 1972. Mechanisms of mesothelioma induction with asbestos and fibrous glass. J Natl Cancer Inst 48:797–821.

Thurston RJ, Hess RA, Kilburn KH, McKenzie WN. 1976. Ultrastructure of lungs fixed in inflation using a new osmium-fluorocarbon technique. J Ultrastruct Res 56:39–47.

Waber U, Im Hof V, Geiser M, Baumann M, Scheuch G, Gebhart J, et al. 1999. A new methodology for controlled particle inhalation by small rodents. Exp Lung Res 22:113–125.

Weibel ER. 1984. Morphometric and stereological methods in respiratory physiology including fixation techniques. In: Techniques in the Life Sciences (Otis AB, ed). County Clare, Ireland:Elsevier Scientific Publishers, 1–35.